Neurocrit Care (2022) 37:302–313
https://doi.org/10.1007/s12028-022-01498-z

NEUROCRITICAL CARE SOCIETY

ORIGINAL WORK

Prognosis After Cardiac Arrest: The Additional Value of DWI and FLAIR to EEG

Hanneke M. Keijzer[1,2*], Marlous M. L. H. Verhulst[1,3], Frederick J. A. Meijer[4], Bart A. R. Tonino[5], Frank H. Bosch[6], Catharina J. M. Klijn[2], Cornelia W. E. Hoedemaekers[7†] and Jeannette Hofmeijer[1,3†]

Abstract

Background: Despite application of the multimodal European Resuscitation Council and European Society of Intensive Care Medicine algorithm, neurological prognosis of patients who remain comatose after cardiac arrest remains uncertain in a large group of patients. In this study, we investigate the additional predictive value of visual and quantitative brain magnetic resonance imaging (MRI) to electroencephalography (EEG) for outcome estimation of comatose patients after cardiac arrest.

Methods: We performed a prospective multicenter cohort study in patients after cardiac arrest submitted in a comatose state to the intensive care unit of two Dutch hospitals. Continuous EEG was recorded during the first 3 days and MRI was performed at 3 ± 1 days after cardiac arrest. EEG at 24 h and ischemic damage in 21 predefined brain regions on diffusion weighted imaging and fluid-attenuated inversion recovery on a scale from 0 to 4 were related to outcome. Quantitative MRI analyses included mean apparent diffusion coefficient (ADC) and percentage of brain volume with ADC < 450×10^{-6} mm^2/s, < 550×10^{-6} mm^2/s, and < 650×10^{-6} mm^2/s. Poor outcome was defined as a Cerebral Performance Category score of 3–5 at 6 months.

Results: We included 50 patients, of whom 20 (40%) demonstrated poor outcome. Visual EEG assessment correctly identified 3 (15%) with poor outcome and 15 (50%) with good outcome. Visual grading of MRI identified 13 (65%) with poor outcome and 25 (89%) with good outcome. ADC analysis identified 11 (55%) with poor outcome and 3 (11%) with good outcome. EEG and MRI combined could predict poor outcome in 16 (80%) patients at 100% specificity, and good outcome in 24 (80%) at 63% specificity. Ischemic damage was most prominent in the cortical gray matter (75% vs. 7%) and deep gray nuclei (45% vs. 3%) in patients with poor versus good outcome.

Conclusions: Magnetic resonance imaging is complementary with EEG for the prediction of poor and good outcome of patients after cardiac arrest who are comatose at admission.

Keywords: Postanoxic coma, Electroencephalography, Magnetic resonance imaging, Diffusion weighted imaging, Cardiac arrest, Prognostication

Introduction

Predicting the neurological recovery of comatose patients after cardiac arrest is challenging. International guidelines recommend a multimodal approach, including clinical examination, electrophysiology, imaging, and biomarkers [1, 2]. Despite application of the multimodal European Resuscitation Council and European Society of Intensive Care Medicine algorithm, neurological prognosis remains uncertain in 50–70% of patients [3–5].

*Correspondence: HMKeijzer@rijnstate.nl
†Cornelia W. E. Hoedemaekers and Jeannette Hofmeijer have contributed equally to this publication.
[1] Department of Neurology, Rijnstate Hospital, P.O. box 9555, 6800 TA Arnhem, The Netherlands
Full list of author information is available at the end of the article

Springer

Electroencephalography (EEG) has been shown to contribute to reliable prediction of outcome, and promising results for the use of magnetic resonance imaging (MRI) have been reported [4–11]. However, the optimal timing of EEG and MRI differ; predictive value of EEG is highest between 12 and 72 h after cardiac arrest, whereas discrimination on the basis of MRI has shown to be optimal after 2–5 days [4, 7, 10, 12].

Diffusion weighted imaging (DWI) is a technique that reflects cell swelling or cytotoxic edema, which is most prominent at 2–5 days after cardiac arrest [13, 14]. Fluid-attenuated inversion recovery (FLAIR) MRI represents vasogenic edema, which appears at 1–2 days and remains visible after (pseudo) normalization of DWI [15]. In addition, where the EEG is most sensitive to cortical processes, MRI also visualizes deeper structures. This is relevant, since these deeper structures, such as the hippocampi, thalamus, and basal ganglia, are relatively sensitive to energy depletion [16].

Because MRI measures different pathological processes and anatomical locations than EEG, combining EEG and MRI for prognosis after cardiac arrest seems rational. Previous retrospective [14, 17, 18] or post hoc [10] analyses showed potential advantage of combining MRI and EEG for the prediction of outcome. However, these studies were unsystematic regarding timing and execution of EEG and MRI.

The aim of the current study was to estimate the additional value of MRI-DWI and FLAIR on day 2–4 after resuscitation, in addition to continuous, early EEG, for prediction of poor or good outcome of patients who are comatose at admission to the intensive care unit (ICU) after cardiac arrest. The timing of these measurements is optimized to the sensitivity of EEG and MRI for the detection of abnormalities and prediction of outcome.

Methods

We performed a prospective multicenter cohort study on outcome prediction of comatose patients after cardiac arrest on the basis of EEG and MRI. Patients were included from two Dutch hospitals between June 2018 and October 2020: Rijnstate Hospital (Arnhem) and Radboud University Medical Center (Radboudumc) (Nijmegen). The study has been performed in accordance with the ethical standards as laid down in the 1964 Declaration of Helsinki and its later amendments or comparable ethical standards and was approved by the Committee on Research Involving Human Subjects region Arnhem-Nijmegen and registered on ClinicalTrials.gov (identifier: NCT03308305).

Study Population

Consecutive patients were included in the study after permission from their legal representatives within 72 h after cardiac arrest. Inclusion criteria were the following: cardiac arrest on the basis of a cardiac cause, Glasgow Coma Scale ≤ 8 at admission, age ≥ 18 years, and admission to the ICU. Exclusion criteria were pregnancy, life expectancy < 24 h post cardiac arrest, any known progressive brain illness—such as a brain tumor or neurodegenerative disease—preexisting dependency in daily living (Cerebral Performance Category [CPC] 3–4), or a contraindication to undergo MRI examination (e.g., presence of pacemaker, neurostimulator, foreign metal objects).

Standard of Care

Patients were monitored and treated according to international guidelines for comatose patients after cardiac arrest. Targeted temperature management at 36 °C (Rijnstate Hospital) or 32–34 °C (Radboudumc) was induced as soon as possible after arrival at the ICU and maintained for 24 h. After 24 h, passive rewarming was controlled at a speed of 0.25–0.5 °C per hour. On rewarming, normothermia was actively maintained. Patients generally received a combination of propofol, midazolam, morphine, or sufentanil for sedation and analgesia.

Decisions on Withdrawal of Treatment

Withdrawal of life sustaining treatment (WLST) was considered at ≥ 72 h after cardiac arrest, during normothermia, and off sedation. Decisions on WLST were on the basis of European guidelines including incomplete return of brainstem reflexes, treatment-resistant myoclonus, and bilateral absence of somatosensory evoked potentials [19]. Treating physicians used the EEG to allow detection and treatment of electrographic epileptic seizures. Since April 2019, the EEG is part of the Dutch guideline "prognosis after postanoxic coma" [20]. The EEG was evaluated daily by a trained neurologist, and results were added to the patients' medical file. We were reserved to use these results in decisions regarding WLST for patients included in this study. However, we cannot fully exclude that the early EEG was taken into account when WLST was considered in some patients, but always > 72 h after the arrest and in a multimodal prediction protocol.

The MRI acquisitions were screened for structural abnormalities and incidental findings, as stated in local research obligations. Radiologists only evaluated the "standard" clinical sequences, i.e., the DWI, FLAIR and T1 sequence. A report was added to the patients' medical

file, but never taken into account in decisions regarding treatment withdrawal.

Outcome

Outcome was assessed at 3 months after cardiac arrest by a standardized telephone interview on the basis of the EuroQol-6D questionnaire by one of two researchers (HMK, MMLHV) blinded to EEG and MRI readings. The primary outcome measure was neurological outcome expressed as the CPC score at 3 months after cardiac arrest. Outcome was dichotomized as "good" (CPC 1–2) or "poor" (CPC 3–5).

Data acquisition

EEG

Continuous EEG recordings were started as soon as possible after arrival at the ICU, always within 24 h after cardiac arrest, and continued for at least 3 days or until patient awakening, as part of standard care. At Rijnstate Hospital, 21 electrodes were placed on the scalp according to the international 10–20 system. At Radboudumc, ten electrodes were used, according to a reduced montage [21]. See Table E1 for hardware specifications.

MRI

All patients underwent a 3 T MRI examination at 3 ± 1 days after cardiac arrest (Philips Ingenia [Rijnstate] or Siemens Skyra [Radboudumc]). The scanning protocol included three-dimensional T1, FLAIR, DWI, and diffusion tensor imaging (DTI) sequences. Details of the sequences are listed in Table E2.

Data analyses

EEG Analysis

A computer algorithm selected 5-min artifact-free EEG epochs at 6, 12, 24, 36, 48, and 72 h after cardiac arrest [22]. EEG epochs were filtered with a sixth order zero-phase Butterworth bandpass filter with a frequency range of 0.5–35 Hz.

EEG analyses were performed offline after the registrations. Anonymized epochs were presented to two reviewers independently (HMK, MMLHV) by the computer, randomly. Reviewers were blinded to the timing of the epoch, the patient's clinical status, medication, and outcome. In case of disagreement, consensus was determined by consultation of a third reviewer (JH).

EEG patterns within the selected epochs were classified as suppressed with or without superimposed synchronous activity, continuous, or other patterns indicative of either good, poor, or indeterminate outcome (Table 1) [4]. In case no epoch was available at a certain time point, we classified the EEG as "indeterminate."

Visual MRI Analysis

Visual MRI analysis was on the basis of DWI and FLAIR. DWI images were reconstructed from the DTI sequence in the first seven patients, and from a dedicated DWI image in the patients included thereafter. Two neuroradiologists (FJAM, BART) independently scored all DWI and FLAIR scans, blinded to the patient's clinical status, medication, and outcome. We used a previously published semiquantitative scoring system of predefined brain regions on a scale from 0 (no damage) to 4 (severe damage due to cardiac arrest) [23]. Consensus was sought when the difference between the scores of the two reviewers was > 1 per brain region, otherwise, the average score was used for that region.

The DWI (range 0–84), FLAIR (0–84), deep gray nuclei (DGN) (0–32), and cortex scores (0–48) were calculated by adding up all scores of the corresponding brain regions as shown in Fig. 1. The overall score is the sum of all brain regions of both DWI and FLAIR (range 0–168). An overall score > 43 and a cortex score > 27 have previously been associated with 100% poor outcome [23].

Table 1 Overview of the EEG categories with corresponding EEG patterns for visual EEG classification

EEG category	Explanation	Indicative to
Suppressed patterns	Continuously supressed EEG, defined as an amplitude < 10 μV	Poor outcome when measured ≥ 24 h post cardiac arrest
Synchronous on suppressed background patterns	Synchronous burst-suppression, with generalized, abrupt-onset bursts or identical bursts with suppressed background activity (≥ 50% suppressions[a]), or generalized periodic discharges with suppressed background activity	Poor outcome when measured ≥ 24 h post cardiac arrest
Continuous patterns	Continuous or nearly continuous activity: maximum amplitude ≥ 20 μV, < 10% suppressions	Good outcome when measured ≤ 12 h post cardiac arrest
Other patterns	Low voltage (maximum amplitude 10–20 μV), epileptiform on other background, burst-suppression (heterogeneous with ≥ 50% suppressions[a]), and discontinuous (10–49% suppressions[a])	Indeterminate outcome

EEG, electroencephalography

[a] Suppressions are defined as segments with amplitude < 10 μV or segments with amplitude ≥ 10 μV, but < 50% of background/burst voltage [4]

Quantitative MRI analysis

Quantitative MRI analysis was on the basis of apparent diffusion coefficient (ADC) maps derived from DTI sequences. Preprocessing of the DTI data consisted of denoising and removal of Gibss artifacts (MRtrix version 3.0), followed by Eddy current and motion correction (FSL; v6.0.2 [24]). Then, the preprocessed data were fitted to a DTI model implemented in MATLAB (v.2016a; The MathWorks Inc) [25]. Here, the ADC map is the equivalent of the mean diffusivity, uncorrected for free water [26]. All voxels with ADC $< 200 \times 10^{-6}$ or $> 2{,}000 \times 10^{-6}$ mm^2/s were removed to exclude artifacts and influence of cerebral spinal fluid (CSF) [8, 14, 27].

From T1 images, eroded whole brain masks were created using FSL's Brain Extraction Tool (BET) [28]. Regional anatomic masks of gray matter (GM) and white matter (WM) were created using the Freesurfer image analysis suite "recon-all" command (version 7.1.1 [29, 30]), and registered to the subject specific DTI space using linear registration (FSL-FLIRT [31]). Mean ADC values of the whole brain, GM, and WM, and proportions of brain tissue with ADC $< 650 \times 10^{-6}$, $< 550 \times 10^{-6}$, or $< 450 \times 10^{-6}$ mm^2/s, were calculated using FSL and in-house created MATLAB scripts.

The semiquantitative scoring of DWI and FLAIR, and quantitative evaluation of the ADC maps for research purposes took place after treatment of the patients was finished. These results were not communicated to the treatment team.

Statistical Analyses

Data are presented as medians with interquartile rages. To compare patients with good and poor outcome on a group level, we used χ^2 tests for ordinal, and Mann–Whitney *U* tests for continuous variables. Interrater agreement was calculated using the weighted Cohen's Kappa.

Predictive values were evaluated using receiver operating characteristics, area under the curve, and sensitivity (95% confidence interval [CI]) at 100% specificity for prediction of poor outcome, and sensitivity (95%CI) at 90% specificity for prediction of good outcome. Thresholds for prediction of poor and good outcome at these specificity levels were derived from receiver operating characteristics analyses, and compared to values reported in previous literature.

p values < 0.05 were assumed statistically significant. Statistical analyses were performed using R version 3.5.3 or MATLAB.

Results

We screened 261 patients for eligibility and received informed consent for 64. Of these, 14 participants were subsequently excluded, because MRI could not be obtained at 3 ± 1 days after cardiac arrest, mostly because of death or hemodynamic instability (See Fig. E1). Table 2 lists the baseline characteristics of the 50 included patients; 20 (40%) patients had a poor outcome. One patient had a temporary hypotension and one a temporary saturation decrease during transportation. This had no adverse consequences for both patients.

In two patients, the EEG measurement was not performed as a result of logistical reasons, in two other patients the FLAIR and DTI scan were not available because the scan was stopped on request of the patient or relative, and in two others DWI ($n = 2$) or the FLAIR scan ($n = 1$) contained too much noise for interpretation. This resulted in available visual DWI analyses for $n = 48$, ADC analyses for $n = 49$, and visual FLAIR analyses for $n = 47$. A minimum of one MRI sequence (DWI, DTI, or FLAIR) was available for all included patients.

EEG Analyses

Suppressed or synchronized with suppressed background patterns in EEG fragments at > 24 h after cardiac arrest was observed in 3/20 (15%) of the patients with poor outcome and never in 30 patients with good outcome. Continuous EEG in EEG fragments at 6 or 12 h was found in 15/30 (50%) of the patients with good outcome and 1/20 (5%) of those with poor outcome. Hence, based on EEG, poor outcome could be predicted with a sensitivity of 15% (95% CI 3–38%) at a specificity of 100% (95% CI 88–100%). Good outcome could be predicted with a sensitivity of 50% (95% CI 31–69%) at a specificity of 95% (95% CI 75–100%).

MRI Analyses

Visual MRI Analysis: Description of Abnormalities per Brain Area

All visually derived MRI scores differed between patients with good and poor outcome (Table 3; all $p < 0.01$). Examples of DWI and FLAIR scans are provided in Fig. 2. The interrater agreement was moderate, with kappa = 0.70. Figure 3 summarizes DWI and FLAIR abnormalities per brain area, in which "abnormality" is defined as a score of ≥ 2. In general, more lesions were apparent on DWI than on FLAIR. DWI abnormalities were found in 75% of the patients with poor outcome in the cortical gray matter, whereas 40% of patients with poor outcome had abnormalities on FLAIR. Patients with good outcome showed abnormalities in the cortical gray matter on DWI in 7% and on FLAIR in 3%. Abnormalities in the DGN were found in 3% of the DWI and FLAIR scans of patients with good outcome and in 45% of the DWI scans and 30% of the FLAIR scans of patients with poor outcome. The WM and brain stem rarely showed lesions.

Visual MRI Analysis: Predictive Values

Thresholds and corresponding predictive values of all scores are summarized in Table 4. A Cortex + DGN score > 17.2 yielded the highest sensitivity (65%, 95% CI 41–83%) for prediction of poor neurological outcome at 100% specificity. An overall score < 5.2 showed the highest sensitivity for prediction of good outcome (56%, 95% CI 37–76%) at 90% specificity.

We find lower thresholds for prediction of both good and poor outcome than reported in previous literature [23, 32].

Quantitative MRI Analysis

Mean ADC of the GM, volume of ADC < 650, < 550, and < 450×10^{-6} mm^2/s differed significantly between patients with poor and good outcome (Table 3). Figure E2 provides ADC values per study site.

All quantitative MRI measures, except ADC in the WM, yield comparable predictive values for poor neurological outcome (sensitivity of 50–55% at 100% specificity: Table 4). Predictive values for good outcome were limited, with highest sensitivity for the volume of brain with ADC < 450×10^{-6} mm^2/s (31% at 90% specificity) Thresholds for prediction are comparable or lower than previously reported (Table 4 [33]).

Combination of EEG and MRI

EEG correctly predicted poor outcome of 3/20 patients (15%). Thirteen (65%) of the patients with poor outcome met at least one of the cutoff values for visual MRI analyses (Table 4) and 11 (55%) at least one of the ADC thresholds for prediction of a poor outcome. Of all patients, none met all EEG and MRI criteria for poor outcome. Sixteen patients (80%) with poor outcome met at least one of the criteria for prediction of a poor outcome by EEG, visual MRI, or ADC, without false positive results.

EEG predicted good outcome in 15/30 patients (50%) with good outcome and indicated 1 false positive result. This patient with false positive prediction of good outcome survived with CPC 3 at six months. Absence of hypoxic ischemic damage on visual MRI analysis predicted good outcome in 21 patients (70%) and indicated four false positives (one patient with CPC 3, three patients died after WLST). The combined ADC thresholds predicted good outcome in nine patients (30%) and indicated four false positives (all died after WLST). Twenty-four (80%) of the patients with good outcome met at least one of the criteria for prediction of a good outcome by EEG or visual MRI, with seven false positives.

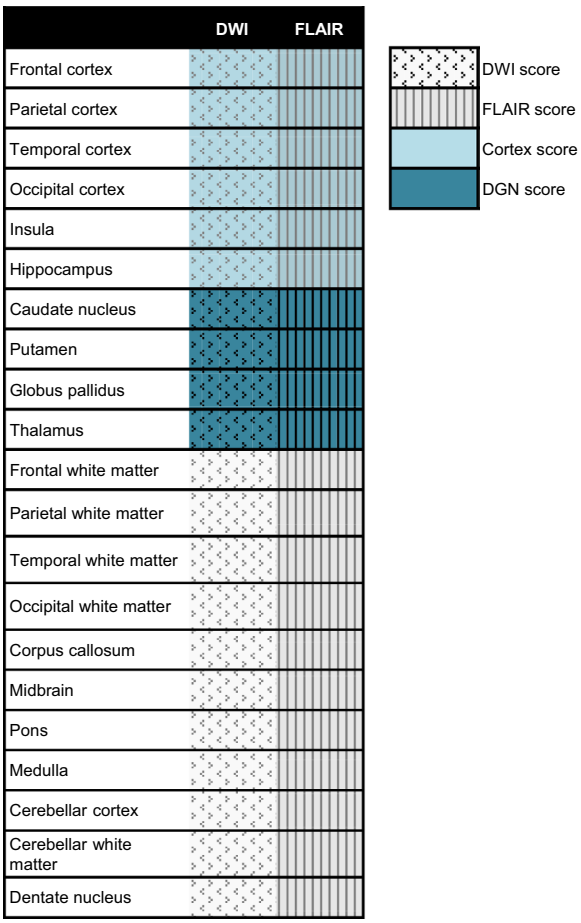

Fig. 1 DWI, FLAIR, cortex, and DGN scores. Individual regions are scored between 0 (no damage) and 4 (severe damage) [23]. The DWI (range 0–84), FLAIR (0–84), DGN (0–32), and cortex scores (0–48) were calculated by adding up all scores of the corresponding brain regions. The overall score is the sum of all brain regions of both DWI and FLAIR (range 0–168). DGN, deep gray nuclei, DWI, diffusion weighted imaging, FLAIR, fluid-attenuated inversion recovery

Discussion

MRI-DWI and FLAIR measured at 3 ± 1 days after cardiac arrest are complementary to EEG for prediction of outcome of patients after cardiac arrest, who are comatose at admission. Combining EEG with visual or quantitative MRI analyses improved reliable prediction of poor or good outcome in this prospective cohort. This emphasizes the value of multimodal outcome prediction, and the need for systematic prospective large studies to develop and validate clinical prediction rules [34]. In comparison with previous, unsystematic, retrospective studies [10, 14, 17, 18], we not only established complementarity of EEG and MRI using a prospective design but also optimized timing of EEG and MRI in a homogeneous population.

The complementary role of EEG and MRI can be understood from a pathophysiological and anatomical

Table 2 Baseline characteristics of patients with good and poor outcome after cardiac arrest

Characteristic	Good outcome ($n = 30$)	Poor outcome ($n = 20$)	p value
Age (yr)	55 (49–57)	70 (64–74)	0.01*
Male sex	25 (83)	14 (70)	0.26
OHCA	30 (100)	20 (100)	NA
Shockable first rhythm	30 (100)	15 (75)	< 0.01*
Duration of resuscitation (min)	12 (10–15)	23 (19–31)	< 0.01*
TTM to 36 °C[a]	22 (73)	17 (85)	0.33
GCS Motor score ≤ 3 at day 3	1 (3)	15 (75)	< 0.01*
SSEP performed	0 (0)	16 (80)	< 0.01*
Bilaterally absent pupillary light response ≥ 72 h	0 (0)	4 (20)	0.01*
Bilaterally absent corneal reflexes ≥ 72 h	0 (0)	5 (25)	< 0.01*
Absent SSEP response	0 (0)	4 (25)	0.01*
EEG indicative to good outcome	15 (50)	1 (5)	< 0.01*
EEG indicative to poor outcome	0 (0)	3 (15)	0.03*
Treatment with propofol	29 (97)	19 (95)	0.77
Average dosage ≤ 24 h (mg/kg/hr)	3.2 (2.7–4.0)	2.5 (2.0–2.9)	< 0.01*
Treatment with midazolam	10 (33)	4 (20)	0.30
Average dosage ≤ 24 h (μg/kg/hr)	72 (47–123)	79 (53–106)	1.0
Treatment with sufentanil	8 (27)	3 (15)	0.33
Average dosage ≤ 24 h (μg/kg/hr)	0.18 (0.13–0.18)	0.09 (0.08–0.10)	0.08
Treatment with morphine	21 (70)	16 (80)	0.43
Average dosage ≤ 24 h (μg/kg/hr)	20 (17–26)	20 (18–25)	0.95
Time ROSC-MRI (hr)	76 (53–9)	75 (65–86)	0.83
Awake during MRI[b]	19 (63)	1 (5)	< 0.01*

Continuous variables are provided as median (interquartile range). Dichotomous variables as n (%). Group differences are calculated using Mann–Whitney U tests or χ^2 tests

EEG, electroencephalography, GCS, Glasgow coma scale, MRI, magnetic resonance imaging, NA, not available, OHCA, out of hospital cardiac arrest, SSEP, somatosensory evoked potential, ROSC, return of spontaneous circulation, TTM, targeted temperature management

*Significant differences

[a] All patients were treated with TTM during the first 24 h, targeted at either 36 °C or 32–34 °C

[b] Awake defined as GCS > 8

perspective: sensitivity to synaptic failure with EEG versus edema on MRI, and measurement of cerebral cortex by EEG versus whole brain by MRI [6, 7, 9]. Contrary to EEG, MRI in comatose patients is not straightforward because every transportation to the radiology department introduces a possible risk for the patient. Four of our initially included patients could not undergo MRI scanning because of hemodynamic instability prior to transportation. In previous studies, 17/27 and 25/112 patients could not undergo MRI because of safety concerns [11, 15]. EEG performed within 12–48 h after cardiac arrest may be used to identify patients with a good or poor neurological prognosis. MRI could be reserved for those patients with remaining prognostic uncertainty, who will benefit most from MRI scanning. This way, unnecessary MRI scanning can be avoided. In previous large studies on EEG based prognosis after cardiac arrest, a suppressed EEG pattern with or without synchronous activity ≥ 24 h after cardiac arrest was invariably associated with a poor outcome [4]. For patients with such EEG patterns, poor outcome can be expected based on the EEG and MRI will likely be of no added value.

On MRI, cortical GM and DGN were more often affected than WM and brain stem. This corresponds with previous studies on brain DWI and postmortem analyses after cardiac arrest [13, 33, 35, 36], and is probably

associated with a relatively high metabolic demand of cerebral gray matter [37] and mitochondrial functioning [38]. The cerebellum may be affected in patients with both good and poor outcome and has little prognostic value. Even though Purkinje cells are sensitive to hypoxia, cerebellar damage mostly leads to symptoms that do not necessarily lead to poor outcome [39].

Interestingly, 7 of the 20 patients with poor outcome were predicted to have a good outcome by either EEG or visual or quantitative MRI analysis. The EEG indicated one patient, who survived with a CPC score of 3. MRI measures indicated six other false positive predictions of good outcome. One, survived with a CPC of 3, two died after WLST, of whom one primarily recovered to a Glasgow Coma Scale of 13. Three other patients died after WLST and showed some form of epileptic activity on the EEG, but no GPDs on a suppressed background. Apparently, severe brain damage can be present in absence of MRI abnormalities or EEG patterns predictive for poor outcome. Absence of prognostic parameters for a poor outcome does not necessarily indicate a good outcome in other predictors as well. For example, presence of N20 responses of the somatosensory evoked potential, is no predictor of a good outcome [2].

Strengths of our study are the prospective design and EEG and MRI measurements in a homogeneous population at standardized and optimized time points. Our study also has limitations. First, as in every study on outcome prediction after cardiac arrest, we cannot exclude possible influence of the self-fulfilling prophecy. To minimize this, WLST was never considered within 72 h after cardiac arrest and never based on brain MRI. Although physicians were not blinded to the EEG, it was never the main argument to stop treatment.

Second, we adjusted our scanning protocol after the first seven patients, to improve signal quality of the DWI. The neuroradiologists only scored severe brain damage in case of clear MRI abnormalities and not in case of any doubt, thus reducing the risk of a false positive prediction of poor outcome. Third we included a relatively small cohort of patients, with a risk of overestimation of predictive values. Additionally, we cannot fully exclude a possible selection bias. Patients' relatives were approached for study participation in an emotionally difficult situation, and only a limited number (25%) gave permission for participation. However, the patient characteristics of our cohort are in line with previously reported larger cohorts, indicating low risk of selection bias.

Table 3 Median and interquartile range of the visual MRI scores and quantitative ADC measures

Measure	Good outcome, median (IQR)	Poor outcome, median (IQR)	*p* value
Visual MRI scores			
Cortex score	2.0 (0.9–4.6)	20.5 (9.3–33.0)	< 0.01
DGN score	0.0 (0.0–0.1)	6.3 (1.5–10.8)	< 0.01
Cortex + DGN score	4 (0.9–7.1)	22.0 (11.8–42.5)	< 0.01
DWI score	2.3 (0.0–6)	20.3 (10.5–30.8)	< 0.01
FLAIR score	1.0 (0.0–4.1)	6.5 (2.3–18.3)	< 0.01
Overall score	4.5 (2.0–9.8)	26.8 (13.3–47.3)	< 0.01
ADC			
Mean ADC[a]	807 (791–820)	765 (704–840)	0.09
GM ADC[a]	847 (826–858)	763 (693–832)	< 0.01
WM ADC[a]	785 (764–806)	758 (672–835)	0.27
Brain volume with ADC < 650[a] (%)	11.9 (8.7–14.4)	23.2 (10.4–38.1)	0.01
Brain volume with ADC < 550[a] (%)	3.0 (2.1–4.4)	10.1 (3.2–20.5)	< 0.01
Brain volume with ADC < 450[a] (%)	0.9 (0.6–1.4)	4.2 (0.9–9.9)	0.01

Group differences are calculated using Mann–Whitney *U* tests, a *p* value < 0.05 is considered significant

ADC, apparent diffusion coefficient, DGN, deep gray nuclei, GM, gray matter, IQR, interquartile range, WM, white matter

[a] ADC values in $\times 10^{-6}$ mm^2/s

The cohort of this study was too small to define and validate criteria on a distinct training and test set. In addition, the number of included variables is relatively large with respect to the size of this cohort. Our reported cutoff values should therefore be considered exploratory and need (external) validation, which also applies to the values reported in previous literature (Table 4). In comparison with a recent study with comparable study design, we chose a minimum specificity of 90% for a prediction for good outcome, where they chose the Youden index or a sensitivity of 100% [33]. This may explain the difference in cutoff values for ADC between these studies. Inconsistencies in visual MRI cutoff values are likely caused by variation in the definition of MRI changes across studies [1]. In our study, only DWI and FLAIR changes caused by recent ischemic damage were graded.

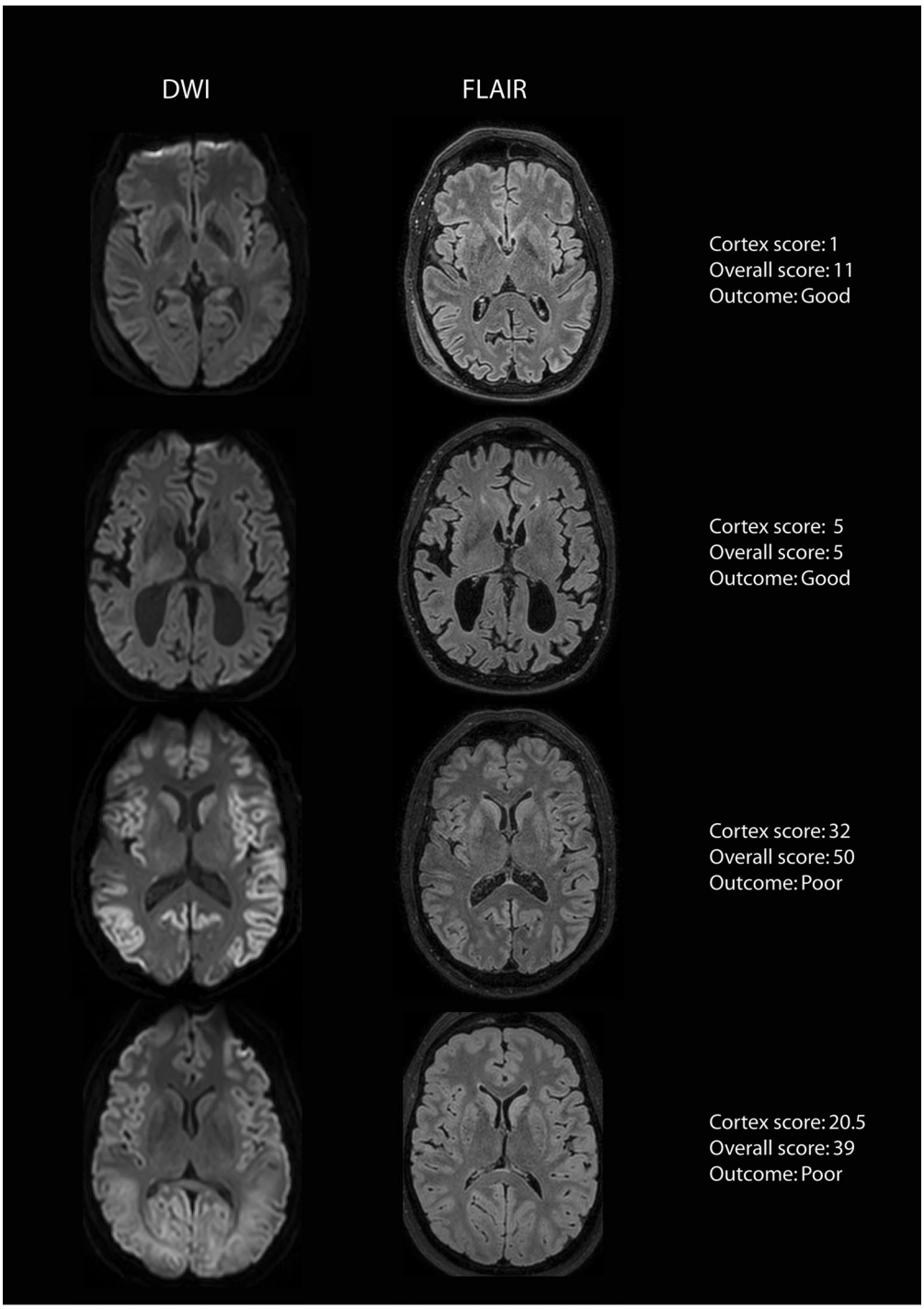

Fig. 2 Example slices of DWI and FLAIR scans of two patients with good outcome and two patients with poor neurological outcome. The cortex score and overall score on the basis of visual grading are reported for each pair. Brain damage on both sequences can be seen as hyperintensities, most prominent in the cortical gray matter and deep gray nuclei for the patients with poor outcome. DWI, diffusion weighted imaging, FLAIR, fluid-attenuated inversion recovery

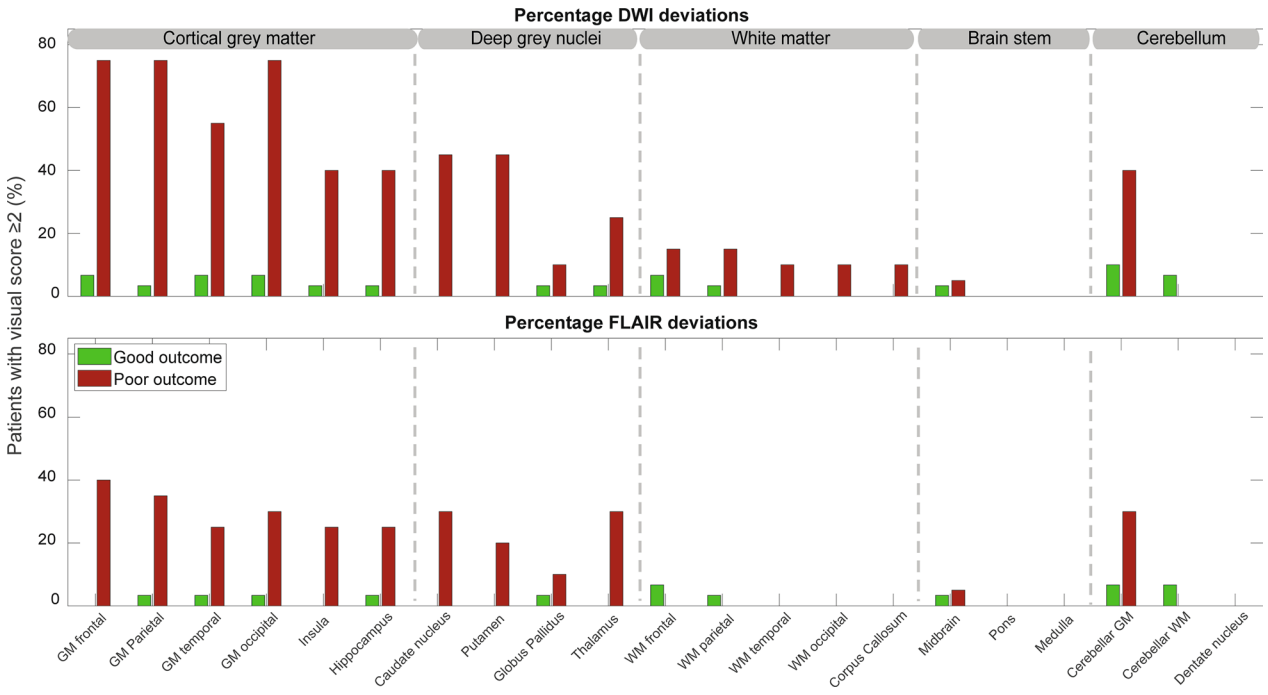

Fig. 3 Percentages of patients with good or poor outcome with abnormalities in the examined brain areas on MRI-DWI and FLAIR images. DWI, diffusion weighted imaging, FLAIR, fluid-attenuated inversion recovery, GM, gray matter, MRI, magnetic resonance imaging, WM, white matter

Although kappa values between radiologists was moderate, some variability may occur in the scoring, for example in the case of small focal lesions in large brain areas, such as the temporal cortex. Before a semiquantitative scoring system can be implemented in clinical practice, a standard method for assessment of the scans should be communicated. Once this method is available and validated, clinical implementation of DWI and FLAIR seems straightforward, since these sequences are standard practice in most hospitals.

Another limiting factor for implementation of quantitative MRI in clinical practice include differences in MRI hardware and scanning protocols, although the interscanner coefficients of variation for overall GM and WM on ADC and mean diffusivity are relatively low (< 4%) [40]. Our study shows that it is possible to find a cutoff value for ADC maps derived from harmonized DWI protocols, but scanner specific cutoff values might yield more accurate results. Visual interpretation of MRI images is less influenced by intervendor differences, slight reductions in image quality, and presence of old WM lesions and atrophy than quantitative MRI analyses. This may explain the higher accuracy of the visual analyses compared to ADC analyses in this study.

Conclusions

Electroencephalography and MRI are complementary for predicting outcome of comatose patients after cardiac arrest. The EEG can be used to identify patients with an uncertain prognosis, who could benefit from MRI scanning. A standardized scoring methodology and validation of our results are necessary before implementation in clinical practices.

Table 4 Predictive values with 95% confidence intervals for good and poor neurological outcome based on the semiquantitative DWI and FLAIR scores and on quantitative ADC analyses

Measure	Previous literature[a]		Results from this study: prediction of good outcome				Results from this study: prediction of poor outcome			
	Threshold for good outcome	Threshold for poor outcome	Threshold	Sensitivity, % (CI)	Specificity, % (CI)	AUC, value (CI)	Threshold	Sensitivity, % (CI)	Specificity, % (CI)	AUC, value (CI)
Visual MRI										
Cortex score	≤10	> 27–30	< 2.4	52 (32–71.7)	90 (66–100)	0.85 (0.68–0.94)	> 17.2	55 (30.8–76.5)	100 (100–100)	0.85 (0.69–0.94)
DGN score	NA	> 16	0.14	0 (0–0)	100 (100–100)	0.87 (0.74–0.96)	> 7	45 (23.8–70.7)	100 (100–100)	0.87 (0.73–0.96)
Cortex + DGN	NA	> 36–41	< 2.5	44 (25–65.2)	90 (65–100)	0.87 (0.7–0.96)	> 17.8	65 (40.8–83.3)	100 (100–100)	0.87 (0.71–0.96)
DWI score	NA	> 27	< 1.8	39.3 (21.2–56)	95 (77–100)	0.87 (0.7–0.96)	> 16.7	55 (30–75.4)	100 (100–100)	0.87 (0.69–0.96)
FLAIR score	NA	> 22	< 0.84	37 (20–57.1)	90 (69–100)	0.79 (0.64–0.9)	> 10.7	35 (15.8–58.7)	100 (100–100)	0.79 (0.64–0.91)
Overall score	NA	> 41–43	< 5.22	56 (36.8–76.3)	90 (69–100)	0.85 (0.7–0.95)	> 27.4	50 (28.6–73)	100 (100–100)	0.85 (0.68–0.95)
Quantitative MRI										
Mean ADC[b]	> 930	< 600–750	> 852	3.4 (0–17.2)	90 (70–100)	0.65 (0.42–0.84)	< 760	50 (26.7–71.4)	100 (100–100)	0.65 (0.39–0.82)
Mean GM ADC[b]	> 923	NA	> 881	6.9 (0–21.4)	90 (69–100)	0.76 (0.57–0.89)	< 802	55 (33.3–78)	100 (100–100)	0.76 (0.58–0.9)
Mean WM ADC[b]	NA	NA	> 886	0 (0–0)	90 (68.4–100)	0.59 (0.36–0.78)	< 720	35 (15.8–58.3)	100 (100–100)	0.59 (0.39–0.79)
Volume ADC < 650[b]	NA	> 10%–23%	< 6.1%	10.3 (3.2–26.1)	90 (70–100)	0.71 (0.51–0.87)	> 21.8%	50 (27.5–71.4)	100 (100–100)	0.71 (0.52–0.86)
Volume ADC < 550[b]	NA	> 6%	< 1.7%	20.7 (8–38.1)	90 (68–100)	0.76 (0.57–0.89)	> 8.0%	55 (33.3–76.6)	100 (100–100)	0.76 (0.58–0.9)
Volume ADC < 450[b]	< 6.5%	NA	< 0.64%	31 (17.2–50)	90 (69–100)	0.74 (0.55–0.89)	> 3.2%	55 (31.3–76.5)	100 (100–100)	0.74 (0.56–0.89)

ADC, apparent diffusion coefficient, AUC, area under the curve, CI, confidence interval, DGN, deep gray nuclei, DWI, diffusion weighted imaging, FLAIR, fluid-attenuated inversion recovery, GM, gray matter, MRI, magnetic resonance imaging, NA, not available, WM, white matter

[a] Thresholds for visual MRI scores from [23, 32], thresholds for ADC values from [8, 13, 14 27, 33, 41]

[b] ADC values in $\times 10^{-6}$ mm^2/s

Supplementary Information
The online version contains supplementary material available at https://doi.org/10.1007/s12028-022-01498-z.

Author details
[1] Department of Neurology, Rijnstate Hospital, P.O. box 9555, 6800 TA Arnhem, The Netherlands. [2] Department of Neurology, Donders Institute for Brain, Cognition, and Behaviour, Radboud University Medical Centre, Nijmegen, The Netherlands. [3] Department of Clinical Neurophysiology, Faculty of Science and Technology, University of Twente, Enschede, The Netherlands. [4] Department of Radiology and Nuclear Medicine, Radboud University Medical Centre, Nijmegen, The Netherlands. [5] Department of Radiology, Rijnstate Hospital, Arnhem, The Netherlands. [6] Department of Intensive Care Medicine, Rijnstate Hospital, Arnhem, The Netherlands. [7] Department of Intensive Care Medicine, Radboud University Medical Centre, Nijmegen, The Netherlands.

Acknowledgements
The authors thank Ruud van Kaam, technical physician at the intensive care unit (ICU) of the Radboudumc, Yvonne Teitink, and Helene Vogelensang, research nurses of the ICU at the Rijnstate Hospital, together with the staff of the ICU, radiology, and clinical neurophysiology departments, for constructive assistance in obtaining informed consent and performing electroencephalography measurements and magnetic resonance imaging examinations.

Author contributions
Conception and design of study and analyses: HMK, MMLHV, FJAM, CWEH, CJMK, and JH. Data collection: HMK, MMLHV, FHB, and CWEH. Data analyses: HMK, MMLHV, FJAM, BART, and JH. Writing of the article (first draft): HMK. Revising of the article: HMK, MMLHV, FJAM, BART, FHB, CWEH, CJMK, and JH. All authors approve of the final manuscript.

Sources of Support
HMK is funded by the Rijnstate-Radboud promotion fund. CJMK is supported by a clinical established investigator grant of the Dutch Heart Foundation (Grant Number 2012T077) and an ASPASIA grant from The Netherlands Organization for Health Research and Development, ZonMw (Grant Number 015008048). JH is supported by a clinical established investigator grant of the Dutch Heart Foundation (Grant Number 2018T070).

Conflicts of interest
The authors report no conflict of interest.

Ethical approval/informed consent
The study is conducted in accordance with ethical standards as laid down in the 1964 Declaration of Helsinki and its later amendments or comparable ethical standards. The study was approved by the Committee on Research Involving Human Subjects region Arnhem-Nijmegen.

Clinical trial registration
ClinicalTrials.gov: NCT03308305

Publisher's Note

Received: 19 October 2021 Accepted: 28 March 2022
Published: 25 April 2022

References

1. Sandroni C, D'Arrigo S, Cacciola S, et al. Prediction of poor neurological outcome in comatose survivors of cardiac arrest: a systematic review. Intensive Care Med. 2020;46(10):1803–51.
2. Nolan, J.P., Sandroni, C., Bottiger, B.W., et al. European Resuscitation Council and European Society of Intensive Care Medicine guidelines 2021: post-resuscitation care. Intensive Care Med 2021.
3. Bongiovanni F, Romagnosi F, Barbella G, et al. Standardized EEG analysis to reduce the uncertainty of outcome prognostication after cardiac arrest. Intensive Care Med. 2020;46(5):963–72.
4. Ruijter BJ, Tjepkema-Cloostermans MC, Tromp SC, et al. Early electroencephalography for outcome prediction of postanoxic coma: A prospective cohort study. Ann Neurol. 2019;86(2):203–14.
5. Westhall E, Rossetti AO, van Rootselaar A-F, et al. Standardized EEG interpretation accurately predicts prognosis after cardiac arrest. Neurology. 2016;86(16):1482–90.
6. Hofmeijer J, Beernink TMJ, Bosch FH, et al. Early EEG contributes to multimodal outcome prediction of postanoxic coma. Neurology. 2015;85(2):137–43.
7. Spalletti M, Carrai R, Scarpino M, et al. Single electroencephalographic patterns as specific and time-dependent indicators of good and poor outcome after cardiac arrest. Clin Neurophysiol. 2016;127(7):2610–7.
8. Hirsch KG, Fischbein N, Mlynash M, et al. Prognostic value of diffusion-weighted MRI for post-cardiac arrest coma. Neurology. 2020;94(16):e1684–92.
9. Keijzer HM, Hoedemaekers CWE, Meijer FJA, et al. Brain imaging in comatose survivors of cardiac arrest: Pathophysiological correlates and prognostic properties. Resuscitation. 2018;133:124–36.
10. Barth R, Zubler F, Weck A, et al. Topography of MR lesions correlates with standardized EEG pattern in early comatose survivors after cardiac arrest. Resuscitation. 2020;149:217–24.
11. Vanden Berghe S, Cappelle S, De Keyzer F, et al. Qualitative and quantitative analysis of diffusion-weighted brain MR imaging in comatose survivors after cardiac arrest. Neuroradiology. 2020;62(11):1361–9.
12. Keijzer HM, Hoedemaekers CWE. Timing is everything: Combining EEG and MRI to predict neurological recovery after cardiac arrest. Resuscitation. 2020;149:240–2.
13. Mlynash M, Campbell DM, Leproust EM, et al. Temporal and spatial profile of brain diffusion-weighted MRI after cardiac arrest. Stroke. 2010;41(8):1665–72.
14. Bevers MB, Scirica BM, Avery KR, et al. Combination of clinical exam, MRI and EEG to predict outcome following cardiac arrest and targeted temperature management. Neurocrit Care. 2018;29(3):396–403.
15. Wijdicks EF, Campeau NG, Miller GM. MR imaging in comatose survivors of cardiac resuscitation. AJNR Am J Neuroradiol. 2001;22(8):1561–5.
16. Bjorklund E, Lindberg E, Rundgren M, et al. Ischaemic brain damage after cardiac arrest and induced hypothermia–a systematic description of selective eosinophilic neuronal death. A neuropathologic study of 23 patients. Resuscitation. 2014;85(4):527–32.
17. Mettenburg JM, Agarwal V, Baldwin M, Rittenberger JC. Discordant observation of brain injury by MRI and malignant electroencephalography patterns in comatose survivors of cardiac arrest following therapeutic hypothermia. AJNR Am J Neuroradiol. 2016;37(10):1787–93.
18. Beuchat I, Sivaraju A, Amorim E, et al. MRI-EEG correlation for outcome prediction in postanoxic myoclonus: a multicenter study. Neurology. 2020;95(4):e335–41.
19. Nolan JP, Soar J, Cariou A, et al. European resuscitation council and european society of intensive care medicine guidelines for post-resuscitation care 2015: section 5 of the European resuscitation council guidelines for resuscitation 2015. Resuscitation. 2015;95:202–22.
20. *Prognose van postanoxisch coma - Neurofysiologisch onderzoek postanoxisch coma*. 2019 [cited 2020 30–11–2020]; https://richtlijnendatabase.nl/richtlijn/prognose_van_postanoxisch_coma/neurofysiologisch_onderzoek_postanoxisch_coma.html.
21. Tjepkema-Cloostermans MC, Hofmeijer J, Hom HW, Bosch FH, vanPutten M. Predicting outcome in postanoxic coma: are ten EEG electrodes enough? J Clin Neurophysiol. 2017;34(3):207–12.
22. Tjepkema-Cloostermans MC, van Meulen FB, Meinsma G, van Putten MJAM. A Cerebral Recovery Index (CRI) for early prognosis in patients after cardiac arrest. Critical care. 2013;17(5):R252.
23. Hirsch KG, Mlynash M, Jansen S, et al. Prognostic value of a qualitative brain MRI scoring system after cardiac arrest. J Neuroimaging. 2015;25(3):430–7.
24. Jenkinson M, Beckmann CF, Behrens TE, Woolrich MW, Smith SM. FSL. Neuroimage. 2012;62(2):782–90.
25. Pasternak O, Sochen N, Gur Y, Intrator N, Assaf Y. Free water elimination and mapping from diffusion MRI. Magn Resonanc Med. 2009;62(3):717–30.

26. Soares JM, Marques P, Alves V, Sousa N. A hitchhiker's guide to diffusion tensor imaging. Front Neurosci. 2013;7:31.
27. Hirsch KG, Mlynash M, Eyngorn I, et al. Multi-center study of diffusion-weighted imaging in coma after cardiac arrest. Neurocrit Care. 2016;24(1):82–9.
28. Smith SM. Fast robust automated brain extraction. Hum Brain Mapp. 2002;17(3):143–55.
29. Fischl B, Salat DH, Busa E, et al. Whole brain segmentation. Neuron. 2002;33(3):341–55.
30. Segonne F, Pacheco J, Fischl B. Geometrically accurate topology-correction of cortical surfaces using nonseparating loops. IEEE Trans Med Imaging. 2007;26(4):518–29.
31. Jenkinson M, Bannister P, Brady M, Smith S. Improved optimization for the robust and accurate linear registration and motion correction of brain images. Neuroimage. 2002;17(2):825–41.
32. Velly L, Perlbarg V, Boulier T, et al. Use of brain diffusion tensor imaging for the prediction of long-term neurological outcomes in patients after cardiac arrest: a multicentre, international, prospective, observational, cohort study. Lancet Neurol. 2018;17(4):317–26.
33. Wouters A, Scheldeman L, Plessers S, et al. Added value of quantitative apparent diffusion coefficient values for neuroprognostication after cardiac arrest. Neurology. 2021;96(21):e2611–8.
34. Nolan JP, Berg RA, Bernard S, et al. Intensive care medicine research agenda on cardiac arrest. Intensive Care Med. 2017;43(9):1282–93.
35. van Putten M, Jansen C, Tjepkema-Cloostermans MC, et al. Postmortem histopathology of electroencephalography and evoked potentials in postanoxic coma. Resuscitation. 2019;134:26–32.
36. Endisch C, Westhall E, Kenda M, et al. Hypoxic-ischemic encephalopathy evaluated by brain autopsy and neuroprognostication after cardiac arrest. JAMA Neurol. 2020;77(11):1430–9.
37. Attwell D, Laughlin SB. An energy budget for signaling in the grey matter of the brain. J Cereb Blood Flow Metab. 2001;21(10):1133–45.
38. Medvedeva YV, Ji SG, Yin HZ, Weiss JH. Differential vulnerability of CA1 versus CA3 pyramidal neurons after Ischemia: possible relationship to sources of Zn2+ accumulation and its entry into and prolonged effects on mitochondria. J Neurosci. 2017;37(3):726–37.
39. Bodranghien F, Bastian A, Casali C, et al. Consensus paper: revisiting the symptoms and signs of cerebellar syndrome. The Cerebellum. 2016;15(3):369–91.
40. Grech-Sollars M, Hales PW, Miyazaki K, et al. Multi-centre reproducibility of diffusion MRI parameters for clinical sequences in the brain. NMR Biomed. 2015;28(4):468–85.
41. Wijman CA, Mlynash M, Caulfield AF, et al. Prognostic value of brain diffusion-weighted imaging after cardiac arrest. Ann Neurol. 2009;65(4):394–402.